Growth of Hydroxyapatite on Sericin Coated and Non-Sericin Coated Silk Fibers using Simulated Body Fluid

Onanong Sukjai[*,], Piyapong Asanithi[*], Supanee Limsuwan[*], Pichet Limsuwan[*,**]**

[*] Applied Nanotechnology Laboratory (ANT Lab), Department of Physics, King Mongkut's University of Technology Thonburi, Bangkok, 10140, Thailand

[**] Thailand Centre of Excellence in Physics, Commission on Higher Education, Ministry of Education, Bangkok, 10140, Thailand

***Abstract*-** Hydroxyapatite (HAp) was grown on sericin coated silk fibers and non-sericin coated silk fibers using simulated body fluid (SBF) at 37 °C and two concentrations of 1.0×standard SBF and 1.5×standard SBF. The results showed that, for both concentrations of SBF, HAp grown on sericin coated silk fibers is more than that on non-sericin coated silk fibers. This indicates that sericin on the silk fiber plays an important role on the growth of HAp on the silk fibers. Moreover, the particle size of HAp grown in 1.5×SBF concentration is smaller than that in 1.0×SBF concentration.

***Index Terms*-** Hydroxyapatite, Simulated body fluid, Sericin, Silk fiber, Concentration, Calcium phosphate

I. INTRODUCTION

The composite material in human body such as bone consists of mineral phase about 70 wt.% and organic matrix about 30 wt.% [1-4]. Mineral phase in natural bone is hydroxyapatite (HAp,$Ca_{10}(PO_4)_6(OH)_2$) which is excellent application in biocompatibility, osteo-conductivity and bioactivity [5]. Nowadays, many applications on such special characteristics of hydroxyapatite have been extensively studied [6] and developed for bone replacement and remodelling processes of cells surrounding soft tissues at the bone-implant interface [7]. HAp may become an excellent host for living tissues since it allows body fluid or human blood to diffuse into its porous structure to supply nutrient and mineral ions for accelerateing the proliferation and differentiation of bone cells [8].

Natural silk fiber, obtained from cocoon *(Bombyx mori)*, consists of protein-based fiber. It is naturally originated from silkworm. There are two types of protein in silk fiber, that is sericin and fibroin. Fibroin is the core filament and benefit for medical applications, substrate for cell culture, artificial skin and tendon [1]. Fibroin was approved for its biocompatibility which can be perfectly used in medical application as reported by Altman [9]. Sericin is naturally coated on the fibroin core. It is a water soluble protein and used in biological and medical applications due to its antibacterial, UV resistant property [10], lipid oxidation [11] and anti-tumour property in immunogenicity [12-13].

In this research, sericin coated silk fibers (SF) and non-sericin coated silk fibers (NSF) were used as seed fibers to induce HAp crystals by soaking in SBF of various concentrations. The silk fibers with induced HAp crystals on the surface were washed and dried for morphological investigation using thermal scanning electron microscopy (SEM) and field-emission electron microscopy (FE-SEM). Then, the deionised (DI) water was added into the silk fibers for sonicating in ultrasonic bath to remove HAp crystals from the silk fibers, and HAp crystals suspended in DI water were obtained. Finally, they were dropped and dried on silicon wafers for characterization. The structure of HAp crystals was characterized by X-ray diffraction (XRD). The element of HAp was characterized by energy dispersive X-ray spectroscopy (EDX). HAp functional group was characterized by Fourier transform infrared spectroscopy (FTIR)

II. EXPERIMENTAL

A. Silk fiber preparation

Two types of silk fibers were prepared: (i) SF and (ii) NSF. SF were prepared by rinsing the raw silk fibers with DI water for three times to remove the dust and impurity on the surface and dried in an oven at 37 °C for 1 day. NSF were prepared by boiling the raw silk fibers in DI water at 100 °C for 20 min and this process was repeated for 5 times to ensure that any residual sericin on the silk fibers was completely removed. Then, both SF and NSF were cut into 5 cm long for soaking in SBF solution.

B. Simulated body fluid preparation

The simulated body fluid (SBF) is the liquid solution that contains the same ion concentrations as human blood plasma as reported by Kokubo [8,14-19]. The 1.5×SBF prepared in this work followed Kokubo's recipe as shown in Table 1. In this work, 1.5×SBF was prepared as a stock solution in which its ion concentration is 1.5 times of human blood. The 1.0×SBF means that the prepared solution has the same ion concentration as in human blood plasma. In this work, the 1.0×SBF was prepared by dilution of 1.5×SBF, following the equation:

$$C_1V_1 = C_2V_2 \qquad (1)$$

where C_1 is the concentration at 1.5×SBF, V_1 is the volume of 1.5×SBF, C_2 is the concentration at 1.0×SBF, V_2 is the volume of 1.0×SBF.

Table 1 Reagent addition order in DI water for 1 litre of 1.5×SBF

Order	Reagent	Source of reagent	Amount

1	NaCl	Ajax Finechem	12.053 [g]
2	$NaHCO_3$	Ajax Finechem	0.533 [g]
3	KCl	Ajax Finechem	0.338 [g]
4	$K_2HPO_4 \cdot 3H_2O$	Carlo Erba Reagent	0.347 [g]
5	$MgCl_2 \cdot 6H_2O$	Ajax Finechem	0.467 [g]
6	1M HCl	J.T. Baker	50 [ml]
7	$CaCl_2$	Ajax Finechem	0.438 [g]
8	Na_2SO_4	Ajax Finechem	0.108 [g]
9	$C_4H_{11}NO_3$ (Tris)	Ajax Finechem	9.177 [g]
10	1M HCl	J.T. Baker	8.5 [ml]

C. Growth of Hap on silk fibers

The prepared 1.0× SBF was filled in two plastic tubes and 1.5×SBF was also filled in another two plastic tubes, each tube with 30 ml. Two types of silk fibers, SF and NSF which already prepared and cut into 5 cm long were used for soaking in SBF solutions.

0.2 g of SF was soaked in 1.0×SBF and 1.5×SBF are SF 1.0 and SF 1.5, respectively. 0.2 g of NSF after soaked in 1.0×SBF and 1.5×SBF are NS F1.0 and NS F1.5, respectively.

The prepared four samples, i.e. SF 1.0, SF 1.5, NSF 1.0 and NSF 1.5 were kept in an incubator at 37°C for 7 days to observe the growth of HAp on the silk fibers. After 7 days, HAp crystals were grown on the surface of all four samples. They were then washed with DI water and dried in an air oven at 37°C for 1 day.

All four dried samples with HAp crystals on the surface were used for investigating the morphology by thermal SEM and FE-SEM. Subsequently, HAp crystals on the silk fibers were removed by sonicating method. About 0.2 g each of four dried silk fibers with HAp crystals on the surface obtained above, was put in 10 ml of DI water and sonicated in ultrasonic bath for 30 min. Then, the silk fibers were removed out of the DI water and small size of HAp crystals suspended in the DI water was obtained. Finally, they were centrifuged at 14,000 rpm for 1 hr and the supernatant was removed out of the tube. The wet HAp crystals were left at the bottom of the tube. About 50 μ l of the wet HAp crystals was dropped on silicon wafers (100) and dried at 70 °C for 20 min. To increase the HAp film, the drop-dried method was repeated for 3 times. The dried HAp samples were used for XRD investigation.

To compare HAp crystals obtained from the growth on the silk fibers with those of pure HAp crystals, therefore pure HAp crystals were also prepared in this work. First, mixing 10.32 g $Ca(OH)_2$ with 120 g DI water. Then, 9.64 g 85 wt% H_3PO_4 solution was added by drop wise into $Ca(OH)_2$ solution. The pH of the mixture was adjusted to be 9.0 by adding ammonium hydroxide and stirred at 800 rpm for 3 hours, followed by three cycles of alternate centrifugation and water-washing to harvest the precipitates. The precipitates were dried in vacuum at 50 °C for 48 hours and ground into fine powder using an agate mortar [22].

D. Characterization

The structure of HAp crystals was characterized by XRD (Rigaku, RING 2000) with CuK_α in the 2θ range of 20°-55° with a scan step of 0.02°. The morphological structure of HAp crystals on the silk fibers was characterized with two methods. First method was thermal SEM (JSM-JEOL, 5800LV) at 10 kV and 10 nm gold coating. Second method was FE-SEM (JSM-JEOL, 6301F) at 5 kV and 30 nm gold coating. The chemical compositions of HAp crystals were analyzed by SEM-EDX (Oxford, ISIS 300) at 10 kV, 30° take off angle and 100 elapsed life times. The functional group of HAp crystals on the silk fibers was characterized using FTIR (Perkin Elmer, Spectrum One) by KBr pellet.

III. RESULTS AND DISCUSSION

Figure 1 shows the XRD patterns of hydroxyapatite ($Ca_{10}(PO_4)_6(OH)_2$) and calcium phosphate ($Ca_3(P_5O_{14})_2$) crystals on SF and NSF. The observed peaks in Figure 1 could be indexed based on HAp and calcium phosphate crystals in Joint Committee on Powder Diffraction Standard (JCPDS) card numbers 09-0432 and 52-1538, respectively.

For NSF, it is seen in Figure 1(a) and 1(b) that mixed crystals of monoclinic phase of calcium phosphate ($Ca_3(P_5O_{14})_2$) and hexagonal phase of HAp ($Ca_{10}(PO_4)_7$) were grown on NSF. However, the grown crystals are mainly calcium phosphates. When the SBF concentration was increased to 1.5×SBF, the XRD pattern shown in Figure 1(b) revealed that more HAp crystals were grown on the silk fibers. For SF, only pure HAp crystals were grown on the silk fibers for both SBF concentrations as shown in Figure 1(c) and 1(d). This grown HAp crystal has the same phase as in human bone. The above XRD results indicate that sericin is an important factor on the growth of HAp crystals on the silk fibers. Sericin composed mainly of serine and aspartic acid compared with glycine and alanine in fibroin. Furthermore, serine and aspartic acid have more COOH group than that of glycine and alanine. COOH group has high electrostatic and hydrophilic force from lone pair electron, therefore it prefers to coordinate with calcium ions (Ca^{2+}) in SBF. As a result, SF is better seed fiber to grow HAp than NSF.

Figure 2 shows the thermal SEM images of crystals on silk fibers. It can be seen in Figure 2(a)-2(d) that the crystals were grown on all silk fiber surfaces. The growth of crystals on silk fibers in Figure 2 because all the prepared SBF solutions used in this work reached a supersaturated concentration. The interfacial energy between a crystal nucleus and silk fiber surfaces in supersaturated concentration is lower than that of the crystals in contact with the SBF solution [21].

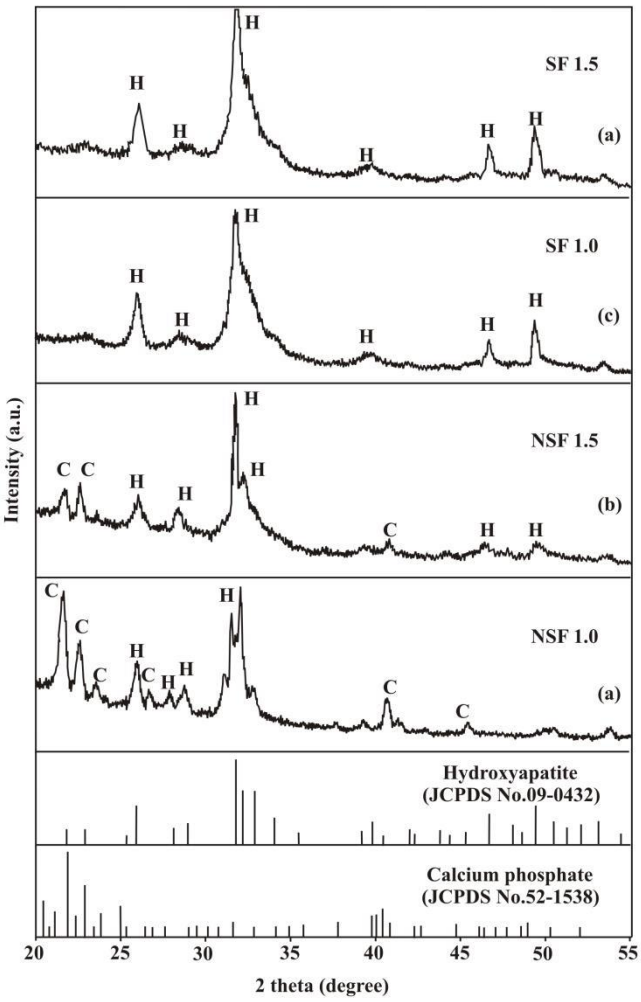

Figure 1 XRD patterns of HAp and calcium phosphate crystals grown on (a) NSF 1.0, (b) NSF 1.5, (c) SF 1.0 and (d) SF 1.5. C is calcium phosphate and H is HAp

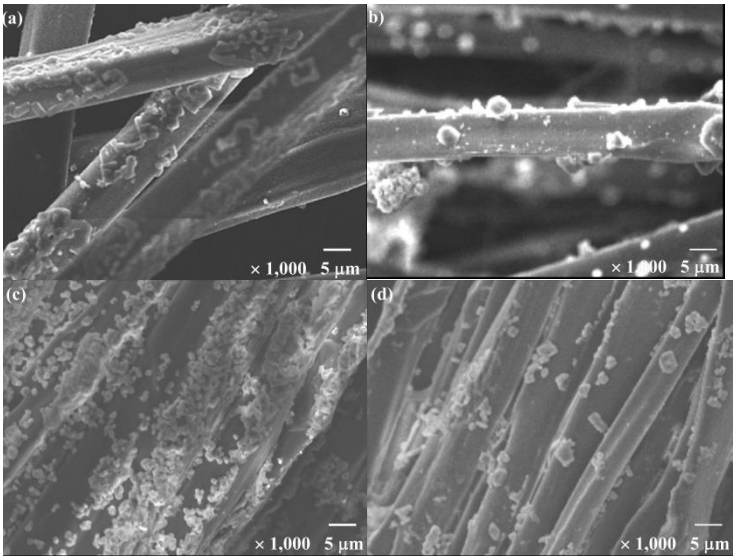

Figure 2 SEM images of crystals on (a) NSF 1.0, (b) NSF 1.5, (c) SF 1.0 and (d) SF 1.5

The above results show that silk fibers are good seed for growing the crystals because there is hydrophilic functional group of protein on silk fibers acted like sponge to absorb SBF. However, we cannot identify the difference between morphology of crystals from thermal SEM images. Therefore, further investigation on crystals was carried out using FE-SEM.

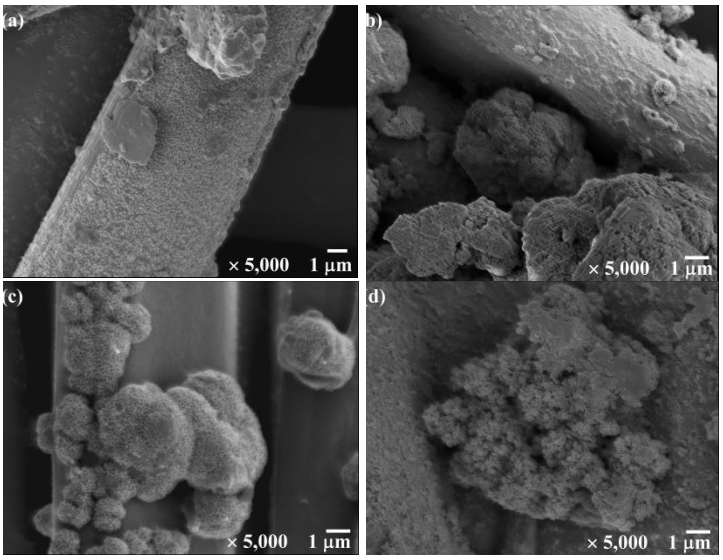

Figure 3 FE-SEM images of calcium phosphate and HAp crystal on (a) NSF 1.0, (b) NSF 1.5, (c) SF 1.0 and (d) SF 1.5

Figure 3 shows the FE-SEM images of the crystals on silk fibers after soaking in SBF. Figure 3(a) and 3(b) show the flat shape and cauliflower shape crystals grown on NSF 1.0 and NSF 1.5, respectively. The flat shape and cauliflower shape crystals are attributed to calcium phosphate and HAp, respectively [23]. These results are in good agreement with those of XRD as shown in Figure 1(a) and 1(b). That is the mixed crystals of calcium phosphate and HAp were grown on both NSF 1.0 and NSF 1.5.

Figure 3(c) and 3(d) show cauliflower shape crystals, that is, HAp, grown on both SF 1.0 and SF 1.5, respectively. The particle size of HAp crystals grown on SF 1.5 and SF 1.5 are in the range of 1-4 μm and 0.1-0.2 μm, respectively. It is seen that the particle size of HAp crystals decreased with increasing SBF concentration. Because at high SBF concentration, that is, high barrier energy is difficult to dilute in solution and hence calcium ions prefer to grow into HAp with small crystals than those of large crystals [21]. The results show that pure HAp crystals were grown only on SF after soaking in both SBF concentrations which agrees well with those of XRD as shown in Figure 1(c) and 1(d).

The chemical composition of cauliflower shape crystals shown in Figure 3(c) was further analyzed by SEM-EDX. The SEM-EDX spectrum of HAp crystals is shown in Figure 4. It is clearly observed that HAp crystals are composed mainly of phosphate and calcium. Oxygen element appeared in SEM-EDX pattern arises from carbonate group of HAp

The functional group of HAp crystals on SF 1.0 was carried out and compared with pure HAp crystals. The IR spectra obtained from HAp crystals growth on SF 1.0 and pure HAp crystals prepared in this work are shown in Figure 5. The

assignments of the vibrational modes associated with different functional groups reported in the literature for HAp crystals is presented in Table 2 [22,24].

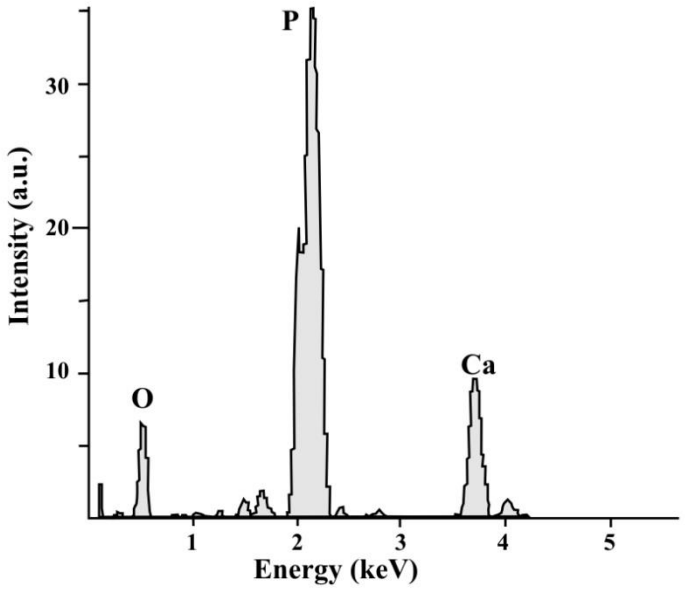

Figure 4 SEM-EDX spectrum of HAp crystals from SF 1.0

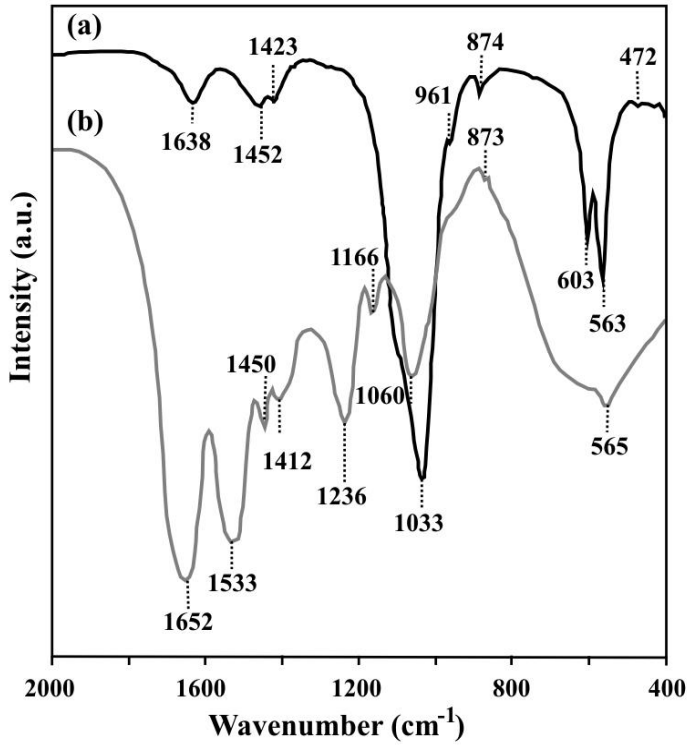

Figure 5 FTIR spectra of (a) pure HAp crystals and (b) HAp crystals on SF 1.0

Table 2 Assignments of infrared vibrational modes of HAp crystals

Frequency (cm^{-1})	Vibrational mode assignments
472-474	ν_2 bending O-P-O
563-565, 602-605	ν_4 bending O-P-O
800-970	ν_2 C-O B
960-965	ν_1 symmetric stretching P-O
1033, 1060	PO_4 group
1165-1167, 1410-1456	Carbonate ion
1230-1410	Amide III
1510-1535	Amide II
1600-1655	Amide I
1610-1640	Bending O-H-O

The peaks located between 472 and 605 cm^{-1} is identified as the bending O-P-O vibration in which the phosphorous move approximately at right angle to the O-O lines and in the O-P-O planes. The peaks at 800-970 cm^{-1} are C-O vibration. The strong peaks at 1033 and 1060 cm^{-1} are PO_4 group [25]. The peaks located between 1165-1167 and 1410-1456 cm^{-1} are carbonate ions [26]. The peaks shown between 1230-1410, 1510-1535 and 1600-1655 cm^{-1} are amide III, amide II and amide I, respectively [27,28]. The peak at 1610-1640 cm^{-1} is bending O-H-O vibration in which the hydrogen move at right angle to the O-O lines and in O-H-O planes. It is clearly observed that the IR spectra of HAp crystals on SF 1.0 showed strong peak of amide I, amide II, and amide III because they are main components in the silk fiber.

The peaks located at 1423 and 1452 cm^{-1} for pure HAp, and 1166, 1412 and 1450 cm^{-1} for HAp crystal on SF 1.0 are derived from carbonate ions, even though no carbonate source was introduced into the starting materials. Since, two samples were prepared in an atmospheric environment, it is reasonable to infer that the carbonate ions incorporated into HAp crystals from carbon dioxide gas in air. The band at 1638 cm^{-1} representing O-H-O bending (OH group) of pure HAp and that of HAp crystals on SF 1.0.

IV. CONCLUSION

This study demonstrates that HAp can be perfectly grown on SF 1.0 and SF 1.5. The structure of HAp as confirmed by XRD was hexagonal, which is the same phase as found in human bone. The morphology of HAp as observed by FE-SEM was confirmed by the cauliflower shape. At a low SBF concentration, NSF 1.0 was not a good seed to induce nucleation of HAp crystals. However, at higher concentration, NSF 1.5 can be used to grow both calcium phosphate and HAp crystals. On the other hand, for SF, they are suitable to be used to grow HAp crystals in both SBF concentrations. Thus, it may be concluded that sericin is a good seed protein for inducing nucleation of HAp crystal. Furthermore, HAp were rapidly grown on SF 1.5 with a small size crystal.

ACKNOWLEDGMENT

This research had partially been supported by Thailand Center of Excellent in Physics (ThEP) and King Mongkut's University of Technology Thonburi under The National Research University Project.

REFERENCES

[1] L. Wang, R. Nemoto, "M Senna, Microstructural and mechanical study of zirconia hydroxyapatite (ZH) composite ceramics for biomedical applications", *J. Eur. Ceram. Soc*. 24 (2004) 2707–2715

[2] K.S. TenHuisen, I.R. Martin, M. Klimkiewicz, P.W. Brown, "Formation and properties of a synthetic bone composite", *J. Biomed. Mater. Res*. 29 (1995) 803-810.

[3] M. Kikuchi, S. Itoh, S. Ichinose, K. Shinomiya, "Self-Organization Mechanism in a Bone-like Hydroxyapatite / Collagen Nanocomposite Synthesized in vitroand Its Biological Reactionin vivo" ,*J. Tanaka, Biomaterials*. 22 (2001) 1705-1711.

[4] C. Du,F.Z. Cui, W. Zhang, Q.L. Feng, X.D. Zhu, K. de Groot, "Formation of calcium phosphate/collagen composites through mineralization of collagen matrix" , *J. Biomed. Mater. Res*. 50 (2000) 518-527.

[5] L. Yucheng, C. Yurong, K. Xiangdong, Y. Juming, "Anisotropic growth of hydroxyapatite on the silk fibroin films", *Applied*. Surf. Sci. 255 (2008) 1681-1685.

[6] R.Z. LeGeros, P.W. Brown, B. Constantz (Eds), "Hydroxyapatite and related Materials", CRC Press, Florida, 1994, 3-28.

[7] S.V. Dorzhkin, " M. Epple, Angew". *Chem. Int. Ed*. 41 (2002) 3130-3140.

[8] T. Kokubo, "Bioceramics and their clinical application", CRC Press, Florida, 2008, pp. 3-24.

[9] G.H. Altman, F. Diaz, C. Jakuba, T. Calabro, R.L. Horan, J. Chen, H. Lu, J.Richmond, D.L. Kaplan, "Silk-based biomaterials", *Biomaterials*. 24 (2003) 401-416.

[10] Y.Q. Zhang, "Applications of natural silk protein sericin in biomaterials", *Biotechnol. Adv*. 20(2002) 91-100

[11] N. Kato, S. Sato, A. Yamanaka, H. Yamada, N. Fuwa, M. Nomura, "Silk protein, sericin, inhibits lipid peroxidation and tyrosinase activity", Biosci. Biotechnol. Biochem. 62 (1998) 145-147.

[12] S. Zhaorigetu, N. Yanaka, M. Sasaki, H. Watanabe, N. Kato, "Inhibitory effects of silk protein, sericin on UVB-induced acute damage and tumor promotion by reducing oxidative stress in the skin of hairless mouse" , *J. Photochem. Photobiol. B. Biol*. 71 (2003) 11-17.

[13] R. Daxh, Ch. Acharya, P.C. Bindu, S.C. Kundu, "Antioxidant potential of silk protein sericin against hydrogen peroxide-induced oxidative stress in skin fibroblasts", *BMB reports*. 41 (2008) 236-240.

[14] T. Kokubo, H. Kushitani, S. Sakka, T. Kitsugi, T. Yamamuro, "Solutiions able to reproduce in vivo surface-structure change in bioactive glass-ceramic A-W", *J. Biomed. Mater. Res*. 24 (1990) 721-734.

[15] T. Kokubo, M. Hanakawa, M. Kawashita, M. Minoda, T. Beppu, T. Miyamoto, T. Nakamura, "Apatite formation on non-woven fabric of carboxymethylate chitin in SBF", *Biomaterials*. 25 (2004) 4485-4488.

[16] M. Uchida, H.M. Kim, F. Miyaji, T. Kokubo, T. Nakamura, "Apatite formation on zirconium metal treated with aqueous NaOH", *Biomaterials*. 23 (2002) 313-317.

[17] Ch. Wu, J. Chang, "Bone like apatite formation on carbon microsphere", *Material Letter*. 61 (2007) 2502-2505.

[18] M. Kawashita, M. Nakao, M. Minoda, H.M. Kim, T. Beppu, T. Miyamoto, T. Kokubo, T. Nakamura, "Apatite-forming ability of carboxyl group-containing polymer gels in a simulated body fluid", *Biomaterials*. 24 (2003) 2477-2484.

[19] L. Yucheng, C. Yurong, K. xiangdong, Y. Juming, "Anisotropic growth of hydroxyapatite on the silk fibroin films", *Appl. Surf. Sci*. 255 (2008) 1681-1685.

[20] G. Saraswathy, S. Pal, C. Rose, T.P. Sastry, "A novel bio-inorganic bone implant containing deglued bone, chitosan and gelatin" , Bull. Mater. Sci. 24 (2001) 415-420.

[21] J.J. De Yoreo, P.G. Vekilov, "Nucleation and growth of cystal", https://secure.hosting.vt.edu/www.geochem.geos.vt.edu/bgep/pubs/Chapter_3_DeYoreo_Vekilov.pdf, pp.57-90.

[22] L. Wang, Ch. Li, "Preparation and physicochemical properties of a novel hydroxyapatite/chitosan-silk fibroin composite" , *Carbohyd. polym*. 68 (2007) 740-745.

[23] C. Zhang, J. Yang, Z. Quan, P. Yang, Ch. Li, Z. Hou, J. Lin, "Hydroxyapatite nano and microcrystals with multiform morphologies: controllable synthesis and luminescence properties", *Cryst. Growth*. Des. 9 (2009) 2725-2733.

[24] S. Markovic, L. Veselinovic, D. Uskokovic, "FTIR Study of Biological Hydroxyapatite" (2010).

[25] S.H. Rhee, J. Tanaka, "Self-assembly phenomenon of hydroxyapatite nanocrystals on chondroitin sulphate" ,*J. Mater. Sci.-Mater. Med*. 14 (2002) 597-600.

[26] I.R. Gibson, W. Bonfield, " Novel synthesis and characterization of an AB-type carbonate substituted hydroxyapatite", *J. Biomed. Mater. Res*. 59 (2002) 697-708.

[27] G. Freddi, P. Monti, M. Nagura, Y. Gotoh, M. Tsukada, "Structure and molecular conformation of tussah silk fibroin films"Effect of heat treatment", *J. Polym. Sci., Part B: Polym. Phys*. 35 (1997) 841-847.

[28] A.V. Mikhonin, Z. Ahmed, A. Ianoul, S.A. Asher, "Assignments and Conformational Dependencies of the Amide III Peptide Backbone UV Resonance Raman Bands", *J. Phys. Chem. B.* 108 (2004) 19020-19028.

AUTHORS

First Author – Onanong Sukjai, Department of Physics, King Mongkut's University of Technology Thonburi, Thailand, onanongsukjai@gmail.com.
Second Author – Dr. Piyapong Asanithi, Department of Physics, King Mongkut's University of Technology Thonburi, Thailand, asanithi@hotmail.com.
Third Author – Assoc. Prof. Dr. Supanee Limsuwan, Department of Physics, King Mongkut's University of Technology Thonburi, Thailand, supanee.lim@kmutt.ac.th.
Fourth Author – Prof. Dr. Pichet Limsuwan, Department of Physics, King Mongkut's University of Technology Thonburi, Thailand, pichet.lim@kmutt.ac.th.

Correspondence Author – Onanong Sukjai, Department of Physics, King Mongkut's University of Technology Thonburi, Thailand, onanongsukjai@gmail.com.